

# Photolysis of iron–siderophore chelates promotes bacterial–algal mutualism

Shady A. Amin<sup>a,1</sup>, David H. Green<sup>b,1</sup>, Mark C. Hart<sup>b</sup>, Frithjof C. Küpper<sup>b</sup>, William G. Sunda<sup>c</sup>, and Carl J. Carrano<sup>a,2</sup>

<sup>a</sup>Department of Chemistry and Biochemistry, San Diego State University, 5500 Campanile Drive, San Diego, CA 92182-1030; <sup>b</sup>Scottish Association for Marine Science, Dunstaffnage Marine Laboratory, Oban, Argyll PA37 1QA, Scotland, United Kingdom; and <sup>c</sup>Beaufort Laboratory, National Oceanographic and Atmospheric Administration, Beaufort, NC 28516

Edited by David M. Karl, University of Hawaii, Honolulu, HI, and approved August 18, 2009 (received for review May 18, 2009)

**Marine microalgae support world fisheries production and influence climate through various mechanisms. They are also responsible for harmful blooms that adversely impact coastal ecosystems and economies. Optimal growth and survival of many bloom-forming microalgae, including climatically important dinoflagellates and coccolithophores, requires the close association of specific bacterial species, but the reasons for these associations are unknown. Here, we report that several clades of *Marinobacter* ubiquitously found in close association with dinoflagellates and coccolithophores produce an unusual lower-affinity dicitrate siderophore, vibrioferrin (VF). Fe-VF chelates undergo photolysis at rates that are 10–20 times higher than siderophores produced by free-living marine bacteria, and unlike the latter, the VF photoproduct has no measurable affinity for iron. While both an algal-associated bacterium and a representative dinoflagellate partner, *Scrippsiella trochoidea*, used iron from Fe-VF chelates in the dark, in situ photolysis of the chelates in the presence of attenuated sunlight increased bacterial iron uptake by 70% and algal uptake by >20-fold. These results suggest that the bacteria promote algal assimilation of iron by facilitating photochemical redox cycling of this critical nutrient. Also, binary culture experiments and genomic evidence suggest that the algal cells release organic molecules that are used by the bacteria for growth. Such mutualistic sharing of iron and fixed carbon has important implications toward our understanding of the close beneficial interactions between marine bacteria and phytoplankton, and the effect of these interactions on algal blooms and climate.**

algal blooms | iron acquisition | vibrioferrin | *Marinobacter* | photochemistry

The growth and species composition of microalgal communities in the ocean are often regulated by the micronutrient iron (1), which in turn influences climate by controlling biogenic calcification, oceanic sequestration of CO<sub>2</sub>, and biological release of dimethyl sulfide (2, 3). Iron may also influence blooms of toxic or harmful algae, which have occurred with increasing frequency in recent decades, and have caused substantial ecological and economic damage worldwide (4). Many bloom-forming algal species, including climatically important dinoflagellates and coccolithophores (2, 3), are known to form beneficial or obligatory close associations with certain bacteria, but the reasons for these associations remain obscure (5–8). The bacteria that closely associate with phytoplankton are believed to be involved in a wide range of interactions, including metabolite/nutrient uptake, provision and remineralization (5, 6), cell differentiation (7), as well as algicidal or bacterioprotective effects (8, 9). To our knowledge, however, these interactions are poorly understood, and only a few well-studied examples exist.

Among the most intriguing factors that may involve algal–bacterial interactions is iron acquisition. Iron is an essential element for photosynthesis and respiration, and it limits primary productivity and bacterial growth in much of the ocean because of its poor solubility and resultant exceedingly low concentration (1, 10, 11). To alleviate limitation of this key micronutrient, many marine heterotrophic bacteria and some cyanobacteria produce siderophores, small organic molecules that tightly bind iron and thereby increase its solubility (12). The bacteria then take up the

siderophores via outer-membrane transporters that are specific for different groups of siderophores. By contrast, eukaryotic phytoplankton are not known to produce siderophores or to directly take up bacterially derived Fe(III)-siderophore complexes. However, many eukaryotic phytoplankton are able to access iron from siderophores or other chelates via ferrireductases and adjacent Fe(II) transporters on their outer cell membranes, for which genomic evidence exists in diatoms and green algae (13).

## Results

We have previously observed that the bacterial community co-occurring with the toxic dinoflagellate *Gymnodinium catenatum* bears a remarkable similarity to the bacterial communities of other marine dinoflagellates from different algal collections (14). Among the most notable members of these communities were bacteria phylogenetically affiliated with the  $\alpha$ -proteobacterial *Roseobacter* and the  $\gamma$ -proteobacterial *Marinobacter* clades. Here, examining a larger set of cultures, we find that members of the genus *Marinobacter* were detected in 83% of dinoflagellate and 87% of the coccolithophorid cultures that we examined, whereas *Marinobacter* spp. were found less frequently in diatom cultures (Tables S1 and S2). These closely related *Marinobacter* spp. have also been cultured from dinoflagellates by others, corroborating the idea that several species of *Marinobacter* are very frequently associated with dinoflagellates and coccolithophores (15, 16).

Although these algal-associated species were closely related to other *Marinobacter* species (e.g., *Marinobacter hydrocarbonoclasticus* or *Marinobacter* sp. DS40M8), most of the tested strains did not produce the siderophores commonly produced by free-living members of the *Marinobacter* genus (12). This observation prompted us to screen many *Marinobacter* isolates for their siderophore production using a combination of liquid chromatography (LC)-MS, NMR, growth promotion assays, and PCR of selected siderophore biosynthetic genes (Fig. 1). The known molecule vibrioferrin (VF) (Fig. 24) was the only siderophore detected in two particular algal-associated subclades, suggesting that: (i) siderophore production may be a useful chemotaxonomic marker for algal-associated *Marinobacter* species, and (ii) there might be some unique functional significance for VF production (17, 18).

VF is a member of the carboxylate class of siderophores containing two  $\alpha$ -hydroxy acid groups. It was originally isolated from *Vibrio parahaemolyticus*, an estuarine enteropathogenic bacterium associated with seafood-borne gastroenteritis (17). We observed

Author contributions: S.A.A., D.H.G., and C.J.C. designed research; S.A.A., D.H.G., and M.C.H. performed research; S.A.A. and D.H.G. analyzed data; and S.A.A., D.H.G., F.C.K., W.G.S., and C.J.C. wrote the paper.

The authors declare no conflict of interest.

This article is a PNAS Direct Submission.

Data deposition: The sequences reported in this paper have been deposited in the GenBank database (accession nos. EU241703–EU241707).

<sup>1</sup>S.A.A. and D.H.G. contributed equally to this work.

<sup>2</sup>To whom correspondence should be addressed. E-mail: carrano@sciences.sdsu.edu.

This article contains supporting information online at [www.pnas.org/cgi/content/full/0905512106/DCSupplemental](http://www.pnas.org/cgi/content/full/0905512106/DCSupplemental).

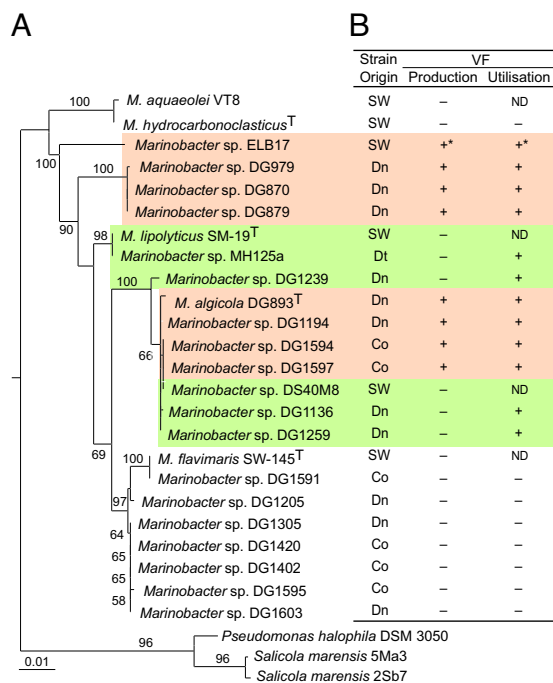


**Fig. 1.** The 16S rRNA gene phylogeny of the *Marinobacter* clade and VF production profile. (A) Maximum-likelihood neighbor-joining tree with bootstrap support ( $\geq 50\%$ ) of *Marinobacter* 16S rRNA genes. (B) Production and utilization of VF by *Marinobacter* for iron acquisition, as determined by LC-MS, NMR, PCR screening of VF biosynthetic genes, and siderophore growth-promotion assays. Dn, dinoflagellate; Co, coccolithophore; Dt, diatoms; ND, not determined. Orange shading indicates those strains capable of VF production and uptake; green shading indicates VF uptake only. Bar denotes nucleotide substitutions per site. \*For *Marinobacter* sp. ELB17, production and uptake were presumed based on the presence of close homologs of VF biosynthetic and uptake genes.

several unique features of VF and its iron chemistry that differed substantially from most other siderophores produced by free living marine bacteria. The first was its only moderate affinity for binding iron (conditional stability constant in seawater (SW) relative to  $Fe^3+$ ,  $\log K^{cond}(FeL, Fe^3) = 10.93 \pm 0.03$ ) owing to the presence of only five iron-binding ligand groups and placing it on par with the weaker class of generic iron binding ligands found in the ocean (19). Most other marine siderophores contain six donor groups, and thus, form much more stable ferric chelates (12). However, the most remarkable feature of VF is the striking sensitivity of its iron complex to light. Siderophores containing  $\alpha/\beta$ -hydroxy acid moieties are known to undergo photochemical reactions involving the oxidative cleavage of a carboxylate group and the concomitant reduction of  $Fe(III)$  to  $Fe(II)$  (20, 21). The  $Fe(II)$  produced can then dissociate from the “degraded” siderophore, and be reoxidized to soluble inorganic ferric hydrolysis species [designated  $Fe(III)'$ ], which are highly bioavailable to algal cells (22, 23). It has been shown that the photolysis of certain ferric chelates and the resultant production of dissolved  $Fe(II)$  and  $Fe(III)'$  species increases the uptake of iron by marine phytoplankton (20, 23). However, the efficiency of this mechanism in increasing the bioavailability of iron is open to question because of the unexpected observation that the photoproducts formed for many photoactive marine siderophores retain the ability to strongly coordinate  $Fe(III)$  (20, 24, 25). Indeed, in some cases, the photoproduct is actually a better  $Fe(III)$  chelator than the parent siderophore (24, 25).

Because VF contains two  $\alpha$ -hydroxy acid moieties, we anticipated that  $Fe(III)$ -VF chelates would be highly photolabile (Fig. 2A), and indeed,  $Fe(III)$ -VF demonstrated exceptional sensitivity to light. It underwent photolysis at a 10- to 20-fold higher rate than

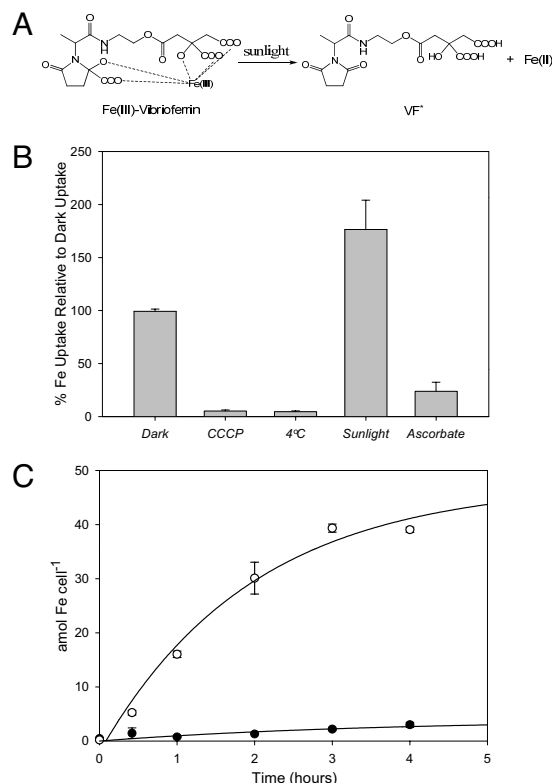


**Fig. 2.** VF-mediated iron uptake in *Marinobacter* sp. DG879 and the dinoflagellate *S. trochoidea* in the dark and in the presence of sunlight. (A) The photolysis of  $Fe(III)$ -VF in sunlight produces a photoproduct ( $VF^*$ ) and  $Fe(II)'$ , which is quickly oxidized in SW to  $Fe(III)'$ . (B)  $^{55}Fe$  uptake rates by *Marinobacter* sp. DG879. Uptake was performed using  $1 \mu M$   $Fe(III)$  and  $3 \mu M$  total VF either in the dark or in the presence of attenuated natural sunlight ( $450 \mu E \cdot m^{-2} \cdot s^{-1}$ ) at  $20^\circ C$ . The uncoupler of oxidative phosphorylation, CCCP, and incubation of cells at  $4^\circ C$  were used as metabolic inhibitors; incubations were carried out in the dark. The reductant ascorbate was used to prevent the oxidation of photochemically produced  $Fe(II)$  in bacteria exposed to sunlight. (C)  $^{55}Fe$  uptake by axenic *S. trochoidea* cells. Uptake was performed in trace-metal- and EDTA-free Aquil using  $50 nM$   $Fe(III)$  and  $500 nM$  VF either in the dark (filled circles) or in the presence of attenuated natural sunlight (open circles) as above. Error bars in B and C represent SD of triplicate cultures. Bars were not shown when smaller than the symbol.

other photoactive siderophores such as petrobactin, marinobactin, and aquachelin (Table 1). Also, unlike any other marine siderophore examined so far, the resulting photoproduct ( $VF^*$ ) (Fig.

**Table 1. Rates of  $Fe(II)$  production during the photolysis of the ferric complexes of VF and other marine siderophores**

Siderophore	Initial specific rate,	Rate of photolysis,	Ref.
	$h^{-1}$ (2,000 $\mu E \cdot m^{-2} \cdot s^{-1}$ )	$h^{-1}$ (80 $\mu E \cdot m^{-2} \cdot s^{-1}$ )	
Vibrioferrin	12.9 (0.017)	0.031	This study
Aquachelin C	0.6 (0.015)	—	20
Petrobactin	—	0.003	This study
Marinobactin	—	<0.001	This study

Initial specific rates were determined by monitoring LMCT of  $Fe^{2+}$ (BPDS) $_3$  at 535 nm as described in *Methods*. BPDS, bathophenanthrolinedisulfonic acid. Values in parentheses represent rates of  $Fe(II)$  production from dark controls. VF photolysis was conducted in natural sunlight attenuated by 75% to an intensity of  $500 \mu E \cdot m^{-2} \cdot s^{-1}$  [1 einstein (E) is 1 mol of photons]; thus, our measured rate was multiplied by a factor of 4 to give the full sunlight rate for comparison with aquachelin C. Rates of photolysis were determined by monitoring changes in the LMCT bands at 330, 490, and 407 nm of the ferric complexes of VF, petrobactin, and marinobactin, respectively, as described in *Methods*.



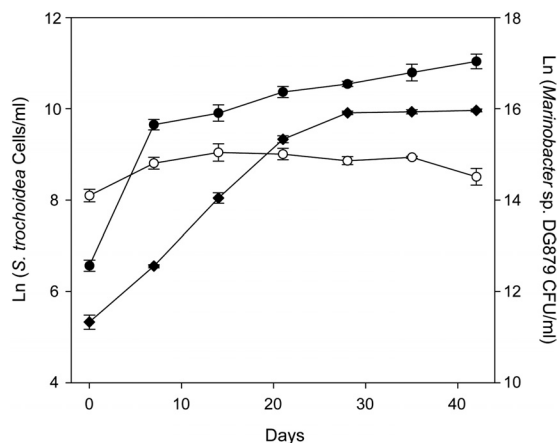


**Fig. 5.** Growth pattern of a binary culture of the bloom-forming *S. trochoidea* and an associated VF-producing *Marinobacter* strain (DG879) in *f2* medium. Growth of *S. trochoidea* (filled diamonds) in the presence of *Marinobacter* sp. DG879 (closed circles) is shown alongside *Marinobacter* sp. DG879 growing alone in *f2* medium (open circles). Error bars represent SD of cell counts from triplicate cultures.

are so widespread. Dinoflagellates are large motile cells ( $\approx 10\text{--}100\ \mu\text{m}$  in diameter), which often migrate vertically between sunlit, nutrient-depleted surface waters during the day, and deeper, more nutrient-enriched waters at night (30). They are positively phototactic, which causes them to accumulate in dense aggregations at the sea surface during the day. It has recently been shown that hydrodynamic effects also tend to force their accumulation into narrow concentrated subsurface layers (31). Such a dense accumulation of algal cells and associated bacteria should lead to more elevated concentrations of VF in the surrounding SW than would occur if the cells were evenly distributed throughout the water column. Together the high photolysis rate constants of Fe-VF chelates, the lack of competing complexation by the photoproduct, and the accumulation of cells near the sea surface should greatly enhance  $\text{Fe(III)}'$  production rates and lead to a highly efficient system for the formation of bioavailable iron. Last, the large size of dinoflagellates causes a further increase in VF concentrations near the cell surface relative to that in the surrounding bulk SW owing to their thick surface diffusive boundary layers (32, 33). The resulting high surface concentrations of VF would help overcome any negative effect of its lower stability constant on its ability to solubilize iron oxides or to compete with the strong iron binding ligands found in SW, whose conditional stability constants ( $3 \times 10^{11}$  to  $1 \times 10^{13}\ \text{M}^{-1}$ ) are higher than those for VF, but whose concentrations are extremely low (1–3 nM) (19).

It is likely that the low stability of ferric VF chelates is not an accident and has been favored by natural selection to make the chelate more readily reducible, both in terms of photoreduction and bioreduction at cell surfaces, which in turn would increase the bioavailability of the iron to the host algal cells (22, 23). There is an inverse relationship between the stability of  $\text{Fe(III)}$  siderophore chelates and their ease of reduction, because high chelate stability energetically favors the maintenance of the bound iron in the +3 oxidation state and discourages its reduction to  $\text{Fe(II)}$  (34). Thus, weakly bound chelates may have been selected evolutionarily in bacterial symbionts to favor iron reduction and iron availability to phytoplankton. There is a tradeoff of course, because if the  $\text{Fe(III)}$  binding is too weak, the chelators will not compete with the strong Fe-binding ligands in SW or with the formation of Fe hydroxides. However, as noted above, dinoflagellates and other algae may have found a way around this difficulty by increasing the ligand concentration in the vicinity of the cells through the formation of dense blooms and the limited diffusive flux of VF [and of photoproducted  $\text{Fe(II)}'$  and  $\text{Fe(III)}'$  species] in the surface boundary layer of the cells.

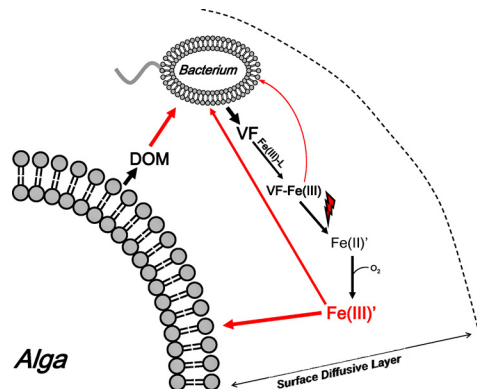


**Fig. 6.** Bacterial–algal mutualism based on the photoreductive dissociation of  $\text{Fe(III)}$ -VF chelates. On binding iron in the light,  $\text{Fe(III)}$ -VF photolyzes to ultimately produce  $\text{Fe(III)}'$ , which is then assimilated by both organisms. In the algae, the assimilated iron is needed in large amounts to support photosynthetic fixation of carbon. Some of this fixed carbon is excreted and used to support bacterial growth and VF production. Due to the thick boundary layer surrounding large algal cells such as dinoflagellates, diffusion of VF and excreted organic carbon away from the algal cell is highly diminished.

Thus, it is evident from our findings that both bacteria and their algal hosts stand to gain in evolutionary selection through close association with one another. The labile iron produced from photolysis of ferric chelates with VF provides iron to the phytoplankton, which need iron in large amounts to support the photosynthetic fixation of carbon. This fixed carbon subsequently fuels the growth and reproduction of both the phytoplankton and their bacterial associates, and is ultimately used to synthesize the siderophore VF (Fig. 6). Such mutualistic sharing of fixed carbon and iron, some aspects of which have been noted earlier (35), has far reaching implications for the biogeochemical cycling of iron and carbon, and the overall influence of phytoplankton and bacteria on each others' evolution. We need a better understanding of these mutualistic interactions if we are to understand and predict the creation of algal blooms and the response of populations of marine algae and bacteria to changes in their environment. Such an understanding is particularly important given the rapid changes now occurring with coastal eutrophication and current and future climate change.

## Methods

**Bacterial Isolation, Culturing, and Growth.** *Marinobacter* spp. were isolated from algal cultures by serial 10-fold dilution and spread-plating on either a low-strength modified Zobell's marine agar (ZM/10) (14) or artificial (A)SW agar (ONR7a) (36) supplied with *n*-hexadecane (Sigma–Aldrich) in the vapor phase as the sole carbon source. Incubation was at room temperature in the dark for 1–4 weeks. Routine culture of *Marinobacter* isolates was on marine agar (2216 or ZM/1) at 30 °C, and cultures were stored frozen at  $-80\ ^\circ\text{C}$  in 20% glycerol.

***Marinobacter* Phylogeny.** Genomic DNA was extracted, and the 16S rRNA gene amplified by PCR according to Green et al. (14). Phylogenetic affiliation was established after automatic alignment by the NAST aligner (<http://greengenes.lbl.gov>) (37) and importation of the aligned sequences into ARB software using the ARB parsimony tool (38). The alignment was refined and ambiguous positions were masked from the analysis. Phylogenetic inference of the masked alignment was based on maximum likelihood (PHYML) using the GTR model of nucleotide substitutions, with bootstrap support (100 resamplings) for nodes, as implemented in ARB. Gamma-proteobacteria of the genus *Salicicola* were used as an outgroup.

**VF Production and Uptake.** VF was isolated as previously described (18) and LC-MS spectra were obtained on a Finnigan LCQ ion-trap mass spectrometer equipped with an ESI source (Finnigan MAT). NMR characterization was carried out on a Varian 500-MHz instrument using standard pulse sequences. Siderophore growth bioassay was performed according to Amin et al. (18).

**Determination of the Inability of the Photoproduct to Bind Fe.** The inability of the photoproduct (VF\*) to coordinate iron was determined by five different methods: (i) the absence of any ligand-to-metal charge-transfer (LMCT) bands in the UV-visible region always observed for Fe(III)-siderophore complexes; (ii) VF\* showed negative results in the universal CAS assay often used to test for siderophores in solution; (iii) at SW pH, VF\* failed to prevent the precipitation of an equimolar amount of Fe(III) as the hydroxide (added as FeCl<sub>3</sub> solution); (iv) in growth-promotion assays, VF\* failed to support the growth of the producing bacteria compared with an equimolar amount of VF, indicating that VF\* is not used as an iron scavenger; and (v) solutions of Fe + VF\* produced by photolysis subjected to HPLC yielded only pure VF\* and not an Fe-VF\* complex.

**PCR Amplification of VF Biosynthetic Genes *pvsAB*.** Degenerate PCR primers were designed to amplify a region between the N terminus of PvsA (PvsA1: GARTGYGAYGTNTTYAAYCC) and C terminus of the PvsB (PvsB1: CCRTARAAYTTRTT-DATRTC), two of the enzymes involved in VF biosynthesis. PCR amplification used standard PCR buffer conditions with 1  $\mu$ M each primer and 2 mM Mg<sup>2+</sup>. Cycling conditions used an initial denaturation step of 94 °C for 5 min, followed by 10-cycle step-down annealing profile starting at 58 °C, extension at 72 °C for 3 min, and denaturation at 94 °C for 10 s, then, a further 30 cycles of annealing at 48 °C (30 s), 72 °C for 3 min, and 94 °C for 10 s, and a final 72 °C for 10-min extension. The expected PCR product was  $\approx$ 3 kbp. PCR products were cloned into pGEM-TEasy (Promega) according to the manufacturer's instructions and sequenced using the forward and reverse M13 sequencing primers and ver 1.1 BigDye terminator chemistry (Applied Biosystems), and electropherograms were obtained by using an ABI 3730xl (Applied Biosystems). Nucleotide sequences were deposited with GenBank under accession numbers EU241703–EU241707.

**Axenic Algal Culture Generation and Growth.** *S. trochoidea* cultures were maintained in f/2 medium prepared with SW collected either from the Santa Barbara Pier or the Tیره passage near Oban, Scotland, and supplemented with selenium (39). They were grown either in borosilicate glass flasks or vented 25-cm<sup>2</sup> tissue culture flasks (Greiner Bio-One). Axenic *S. trochoidea* cultures were generated using a two-stage procedure. Stage 1: *S. trochoidea* CCAP 1134/1 was induced to form sexual resting cysts by growth in f/2 medium deficient in nitrate and phosphate. Cysts were harvested by micropipette, washed in sterile f/2 medium, and surface-sterilized with 0.1% H<sub>2</sub>O<sub>2</sub>. The cysts were then washed with sterile f/2 medium to remove residual H<sub>2</sub>O<sub>2</sub>. The cysts were added to sterile f/2 in Petri dishes (Nunc), to which  $\approx$ 1  $\times$  10<sup>4</sup> colony-forming units per mL of *Marinobacter* sp. DG879 was added, and were allowed to germinate and grow out under standard light and temperatures regimes suitable for *Scrippsiella*. Stage 2: Approximately 1 mL of viable vegetative culture was added to 100 mL of f/2 medium in glass flasks and amended with streptomycin sulfate (30  $\mu$ g·mL<sup>-1</sup>; Sigma-Aldrich), and the culture was grown through to stationary phase. Bacterial presence was monitored weekly by spread-plate technique using ZM/10 agar. Cultures from which bacteria had been eliminated were subcultured by adding 1 mL of the axenic culture to 100 mL of sterile f/2 medium containing streptomycin (30  $\mu$ g·mL<sup>-1</sup>), and the culture was again grown through to stationary phase. Bacterial contamination was then monitored using agar culture, and the absence of PCR product amplified using the universal bacterial primer pair 27f and 1492r was confirmed (40).

All cultures were grown in a Thermo-818 Illuminated incubator at 18 °C with 14:10 light/dark cycle at a photon flux density of 80 microeinstein ( $\mu$ E)·m<sup>-2</sup>·s<sup>-1</sup>. Algal cell counts were routinely monitored using a Trilogy fluorometer (Turner Designs 7200) or using a Sedgwick-Rafter counting slide.

**Algal-Bacterial Binary Culture Growth.** *S. trochoidea* and *Marinobacter* sp. DG879 binary cultures, or *Marinobacter* sp. DG879 alone, were grown in triplicate 100-mL flasks containing f/2 medium prepared with natural SW and amended with selenium (39). The *Marinobacter*-only flasks were inoculated with a suspension of DG879 prepared by resuspending several colonies of DG879 in sterile f/2 medium. *S. trochoidea* and DG879 binary culture flasks were inoculated with 1 mL of stationary-phase binary culture. Growth was at 15 °C with a 12:12 light/dark cycle at a photon flux density of  $\approx$ 80  $\mu$ E·m<sup>-2</sup>·s<sup>-1</sup>. All flasks were sampled weekly. Lugol's fixed *S. trochoidea* cell were enumerated by using a Sedgwick-Rafter chamber. Bacterial colony-forming units were determined by spread-plating 10-fold serial dilutions of *Marinobacter* on ZM/1 agar (14).

**<sup>55</sup>Fe Uptake by *S. trochoidea* and *Marinobacter* sp. DG879.** <sup>55</sup>Fe-VF complex was prepared by adding a standard solution of FeCl<sub>3</sub>·6H<sub>2</sub>O (1 mg/mL; Aldrich) and <sup>55</sup>FeCl<sub>3</sub> (1,522 MBq/mL; Perkin-Elmer) to VF (final Fe:ligand = 1:10 for algal uptake, and 1:3 for bacterial uptake; final FeCl<sub>3</sub>:<sup>55</sup>Fe = 1:0.1) in the dark. The complex was allowed to equilibrate for at least 24 h in the dark before use.

For bacterial iron uptake, cells were grown in ASW (18) with the final pH adjusted to 8.0. The ASW was passed through Chelex-100 resin (Bio-Rad) to remove trace metals and supplemented with 100 nM FeCl<sub>3</sub>. Cultures were har-

vested at midexponential growth phase by centrifuging at 6,000 rpm for 20 min in a Sorvall RC5C+ centrifuge followed by washing three times with iron-free ASW. The harvested cells were then diluted with ASW to an optical density at 600 nm of 0.4 and incubated at 4 °C until further use (24). Before the start of the uptake, cells were shaken at 130 rpm and 20 °C for 30 min, after which the experiment was started by adding a 1  $\mu$ M final <sup>55</sup>FeVF concentration. Ascorbate (10 mM) and carbonyl cyanide 3-chlorophenylhydrazone (CCCP; 30  $\mu$ M) were added 1 h before adding <sup>55</sup>FeVF. Uptake experiments at low temperature or in the presence of CCCP were kept in the dark and maintained at 20 °C. Uptake in the presence of the reductant ascorbate was performed by photolyzing the required amount of <sup>55</sup>FeVF by using a mercury vapor lamp (175 W) for 30 min at acidic pH and in the presence of 10 mM ascorbate before addition to the culture. Cultures not kept in the dark were exposed to attenuated sunlight (450  $\mu$ E·m<sup>-2</sup>·s<sup>-1</sup>) and maintained at 20 °C using a refrigerated circulating water bath (Neslab). Aliquots were withdrawn at each time point and filtered using a Millipore 1225 sampling vacuum manifold onto 0.6- $\mu$ m pore size polycarbonate filters (Millipore). Filtered cells were washed with 5 mL of ASW followed by 5 mL of Ti(III)-citrate-EDTA reagent (41) and a final 5-mL rinse with ASW to reductively remove iron oxides and iron bound to cell surfaces. <sup>55</sup>Fe cellular uptake was measured using a Beckman-Coulter LS6500 liquid scintillation counter.

Axenic *S. trochoidea* cultures used in iron uptake experiments were grown in Aquil (886  $\mu$ M NO<sub>3</sub><sup>-</sup>/36.3  $\mu$ M PO<sub>4</sub><sup>3-</sup>/100  $\mu$ M EDTA/100 nM Fe supplemented as FeEDTA) (42). All cultures were grown in a Thermo-818 Illuminated incubator at 18 °C with 14:10 light/dark cycle at a photon flux density of 80  $\mu$ E·m<sup>-2</sup>·s<sup>-1</sup>. Exponentially growing cells were harvested by gravity filtration into Aquil medium containing no EDTA, vitamins, iron, or other trace metal additions. The culture sample was concentrated by passage of  $\approx$ 90% of the culture medium through a 1.2- $\mu$ m pore polycarbonate filter (Millipore) housed in an acid-washed Nalge polysulfone filter holder followed by redilution of the culture with EDTA and trace-metal-free Aquil medium. This procedure was repeated at least four more times to free the culture of residual EDTA. The final diluted culture contained  $\approx$ 10<sup>4</sup> algal cells per mL. <sup>55</sup>FeVF was then added as previously described for the bacteria, and cultures were either kept in the dark or exposed to attenuated sunlight (450  $\mu$ E·m<sup>-2</sup>·s<sup>-1</sup>). Both cultures were maintained at 20 °C. Aliquots were withdrawn at each time point and filtered onto 3- $\mu$ m pore size polycarbonate filters (Millipore). Sample washings and counts were done as previously described.

**Determination of the Conditional Stability Constant of VF in SW.** To determine the conditional stability constant of VF in SW, 10-mL subsamples of open-ocean surface SW that had been UV-irradiated for 8 h and "chelexed," were aliquoted into acid-cleaned Teflon cups; 1 nM VF was then added to each cup, followed by boric acid buffer (pH 8) and iron additions ranging from 0 to 6 nM. Subsamples were allowed to equilibrate for 2 h before adding 10  $\mu$ M salicylaldehyde (SA). After equilibrating for 15 min with SA, samples were analyzed (three independent titrations) by competitive ligand-exchange adsorptive cathodic stripping voltammetry (CLE-ACSV) according to Buck et al. (43). All titrations were done in the dark to prevent photodegradation of VF. The total dissolved iron concentration in the chelexed, UV-irradiated SW (0.1 nM) was determined via ACSV with SA (43).

**Photolysis of Fe(III)-VF.** Fe(III)-VF (5, 10, and 15  $\mu$ M, three replicates each) solutions containing a 10-fold molar excess of total VF were irradiated in the presence of 20, 40, and 45  $\mu$ M ferrous trapping agent, bathophenanthrolinedisulfonic acid (BPDS; Fluka), respectively. The solutions contained 5 mM HEPES buffer (pH 8.1) and were made up in Aquil (without nutrients, trace metals, EDTA, or vitamins). One set of solutions was exposed to attenuated sunlight (500  $\mu$ E·m<sup>-2</sup>·s<sup>-1</sup>) at 20 °C, whereas a set of control samples was kept in the dark. Initial rates of Fe(II) production were measured by monitoring Fe(BPDS)<sub>3</sub><sup>2+</sup> LMCT band at 535 nm (22,140 M<sup>-1</sup>·cm<sup>-1</sup>). For the low light flux experiment, 0.1 mM ferric complexes of VF, petrobactin, and marinobactin solutions were exposed to a fluorescent lamp (80  $\mu$ E·m<sup>-2</sup>·s<sup>-1</sup>, Sylvania Ecologic Cool White, 34 W) at 20 °C in the presence of 50 mM HEPES buffer (pH 8.2) and 0.7 M NaCl. UV-visible spectra were recorded using a Cary 50 spectrophotometer.

**Ferrireductase Assay.** Axenic *S. trochoidea* was grown in acid-washed 250 mL Erlenmeyer flasks in f/2 supplemented with 10<sup>-5</sup> M Fe. Late log-phase cells were harvested by gentle filtration onto 10- $\mu$ m pore polycarbonate membranes, washed twice with equal volumes of sterile natural SW, and finally suspended in an equal volume of sterile natural SW. Triplicate *S. trochoidea* cell suspensions were incubated at 21 °C in the dark in the presence of 130  $\mu$ M HEPES buffer (pH 8.1), 10  $\mu$ M Fe (chelated with 10-fold excess EDTA), and 100  $\mu$ M of the Fe(II) chelator BPDS. Sterile natural SW was used as a background control. Ferrireductase activity was measured by pelleting the algal cells by centrifugation and

measuring the absorbance of Fe(II)BPDS chelates in the supernatant at a wavelength of 535 nm.

**ACKNOWLEDGMENTS.** We thank C. Bolch and T. Gutierrez for access to additional bacteria isolated from algae and Prof. Kathy Barbeau and Randelle M. Bundy (Scripps Institute for Oceanography, University of California, San Diego) for the measurement of the conditional stability constant of VF in SW. This work was

supported by National Oceanographic and Atmospheric Administration Grants NA04OAR4170038 and NA08OAR4170669, and California Sea Grant College Program Projects R/CZ-198 and R/CONT-205. D.H.G. was supported in part by a New Zealand Foundation for Research, Science, and Technology postdoctoral fellowship. DNA sequencing was supported by a Natural Environment Research Council (London) Molecular Genetics Facility Grant MGF 122 (to D.H.G.). Genome sequencing of *M. algicola* DG893 was supported by the Gordon and Betty Moore Foundation.

1. Coale KH, et al. (1996) A massive phytoplankton bloom induced by an ecosystem-scale iron fertilization experiment in the equatorial Pacific Ocean. *Nature* 383:495–501.
2. Dymond J, Lyle M (1985) Flux comparisons between sediments and sediment traps in the eastern tropical Pacific: Implications for atmospheric CO<sub>2</sub> variations during the Pleistocene. *Limnol Oceanogr* 30:699–712.
3. Keller MD, Bellows WK, Guillard RRL (1989) Dimethyl sulfide production in marine phytoplankton. *Biogenic Sulfur in the Environment*, eds Saltzman ES, Cooper WJ (Am Chem Soc, Washington, DC), pp 167–182.
4. Cloern JE (2001) Our evolving conceptual model of the coastal eutrophication problem. *Mar Ecol Prog Ser* 210:223–253.
5. Cho BC, Azam F (1988) Major role of bacteria in biogeochemical fluxes in the ocean's interior. *Nature* 332:441–443.
6. Croft MT, Lawrence AD, Raux-Deery E, Warren MJ, Smith AG (2005) Algae acquire vitamin B<sub>12</sub> through a symbiotic relationship with bacteria. *Nature* 438:90–93.
7. Matsuo Y, Imagawa H, Nishizawa M, Shizuri Y (2005) Isolation of an algal morphogenesis inducer from a marine bacterium. *Science* 307:1598.
8. Mayali X, Franks PJS, Azam F (2008) Cultivation and ecosystem role of a marine *Roseobacter* clade-affiliated cluster bacterium. *Appl Environ Microbiol* 74:2595–2603.
9. Mayali X, Doucette GJ (2002) Microbial community interactions and population dynamics of an algal bacterium active against *Karenia brevis* (Dinophyceae). *Harmful Algae* 1:277–293.
10. Bruland KW, Donat JR, Hutchins DA (1991) Interactive influences of bioactive trace metals on biological production in oceanic waters. *Limnol Oceanogr* 36:1555–1577.
11. Tortell PD, Maldonado MT, Granger J, Price NM (1999) Marine bacteria and biogeochemical cycling of iron in the oceans. *FEMS Microbiol Ecol* 29:1–11.
12. Vraspir JM, Butler A (2009) Chemistry of marine ligands and siderophores. *Annu Rev Mar Sci* 1:43–63.
13. Kustka AB, Allen AE, Morel FMM (2007) Sequence analysis and transcriptional regulation of Iron acquisition genes in two marine diatoms. *J Phycol* 43:715–729.
14. Green DH, Llewellyn LE, Negri AP, Blackburn SI, Bolch CJS (2004) Phylogenetic and functional diversity of the cultivable bacterial community associated with the paralytic shellfish poisoning dinoflagellate *Gymnodinium catenatum*. *FEMS Microbiol Ecol* 47:345–357.
15. Alavi M, Miller T, Erlandson K, Schneider R, Belas R (2001) Bacterial community associated with *Pfiesteria*-like dinoflagellate cultures. *Environ Microbiol* 3:380–396.
16. Hold GL, et al. (2001) Characterisation of bacterial communities associated with toxic and non-toxic dinoflagellates: *Alexandrium* spp. and *Scrippsiella trochoidea*. *FEMS Microbiol Ecol* 37:161–173.
17. Yamamoto S, Okujo N, Yoshida T, Matsuura S, Shinoda S (1994) Structure and iron transport activity of vibrioferrin, a new siderophore of *Vibrio parahaemolyticus*. *J Biochem* 115:868–874 (in Japanese).
18. Amin SA, Küpper FC, Green DH, Harris WR, Carrano CJ (2007) Boron binding by a siderophore isolated from marine bacteria associated with the toxic dinoflagellate *Gymnodinium catenatum*. *J Am Chem Soc* 129:478–479.
19. Rue EL, Bruland KW (1995) Complexation of Fe(III) by natural organic ligands in the central North Pacific as determined by a new competitive ligand equilibration/adsorptive cathodic stripping voltammetric method. *Mar Chem* 50:117–138.
20. Barbeau K, Rue EL, Bruland KW, Butler A (2001) Photochemical cycling of iron in the surface ocean mediated by microbial iron(III)-binding ligands. *Nature* 413:409–413.
21. Barbeau K (2006) Photochemistry of organic iron(III) complexing ligands in oceanic systems. *Photochem Photobiol* 82:1505–1516.
22. Shaked Y, Kustka AB, Morel FMM (2005) A general kinetic model for iron acquisition by eukaryotic phytoplankton. *Limnol Oceanogr* 50:872–882.
23. Anderson MA, Morel FMM (1982) The influence of aqueous iron chemistry on the uptake of iron by the coastal diatom *Thalassiosira weissflogii*. *Limnol Oceanogr* 27:789–813.
24. Küpper FC, Carrano CJ, Kuhn J-U, Butler A (2006) Photoreactivity of iron(III)-aerobactin: Photoproduct structure and iron(III) coordination. *Inorg Chem* 45:6028–6033.
25. Abergel RJ, Zawadzka AM, Raymond KN (2008) Petrobactin-mediated iron transport in pathogenic bacteria: Coordination chemistry of an unusual 3,4-catecholate/citrate siderophore. *J Am Chem Soc* 130:2124–2125.
26. Shouldice SR, et al. (2004) Structural basis for iron binding and release by a novel class of periplasmic iron-binding proteins found in Gram-negative pathogens. *J Bacteriol* 186:3903–3910.
27. Alexeev D, et al. (2003) A novel protein-mineral interface. *Nat Struct Mol Biol* 10:297–302.
28. Mykkestad SM (1995) Release of extracellular products by phytoplankton with special emphasis on polysaccharides. *Sci Tot Environ* 165:155–164.
29. Worden AZ, Cuvelier ML, Bartlett DH (2006) In-depth analyses of marine microbial community genomics. *Trends Microbiol* 14:331–336.
30. Kamykowski D, Milligan EJ, Reed RE (1998) Relationships between geotaxis/phototaxis and diel vertical migration in autotrophic dinoflagellates. *J Plankton Res* 20:1781–1796.
31. Durham WM, Kessler JO, Stocker R (2009) Disruption of vertical motility by shear triggers formation of thin phytoplankton layers. *Science* 323:1067–1070.
32. Richardson LL, Stolzenbach KD (1995) Phytoplankton cell size and the development of microenvironments. *FEMS Microbiol Ecol* 16:185–191.
33. Jonsson PR, Pavia H, Toth G (2009) Formation of harmful algal blooms cannot be explained by allelopathic interactions. *Proc Natl Acad Sci USA* 106:11177–11182.
34. Lewis BL, et al. (1995) Voltammetric estimation of iron(III) thermodynamic stability constants for catecholate siderophores isolated from marine bacteria and cyanobacteria. *Mar Chem* 50:179–188.
35. Kirchman DL, et al. (2000) Carbon versus iron limitation of bacterial growth in the California upwelling regime. *Limnol Oceanogr* 45:1681–1688.
36. Dyksterhouse SE, Gray JP, Hervig RP, Lara JC, Staley JT (1995) *Cycloclasticus pugetii* gen. nov., sp. nov., an aromatic hydrocarbon-degrading bacterium from marine sediments. *Int J Syst Bacteriol* 45:116–123.
37. DeSantis TZ, et al. (2006) Greengenes, a chimera-checked 16S rRNA gene database and workbench compatible with ARB. *Appl Environ Microbiol* 72:5069–5072.
38. Ludwig W, et al. (2004) ARB: A software environment for sequence data. *Nucleic Acids Res* 32:1363–1371.
39. Guillard RRL (1975) Culture of phytoplankton for feeding marine invertebrates. *Culture of Marine Animals*, eds Smith VL, Chanley MH (Plenum, New York), pp 26–60.
40. Weisburg WG, Barns SM, Pelletier DA, Lane DJ (1991) 16S ribosomal DNA amplification for phylogenetic study. *J Bacteriol* 173:697–703.
41. Hudson RJM, Morel FMM (1989) Distinguishing between extra- and intracellular iron in marine phytoplankton. *Limnol Oceanogr* 34:1113–1120.
42. Price NM, et al. (1988/1989) Preparation and chemistry of the artificial algal culture medium Aquil. *Biol Oceanogr* 6:443–461.
43. Buck KN, Lohan MC, Berger C, Bruland K (2007) Dissolved iron speciation in two distinct river plumes and an estuary: Implications for riverine iron supply. *Limnol Oceanogr* 52:843–855.